Cold-Target Recoil-Ion Momentum Spectroscopy: First Results and Future Perspectives of a Novel High Resolution Technique for the Investigation of Collision-Induced Many-Particle Reactions

In order to investigate many-particle reaction dynamics in atomic collisions, a novel high-resolution technique has been developed, which determines the momentum and the charge state of the slowly recoiling target ions. Using a very cold, thin, and localized supersonic gas jet target, a momentum resolution of better than 0.05 a.u. is obtained by measuring the recoil-ion time-of-flight and the recoil-ion trajectory. Because of the very high detection efficiency of nearly 100% this technique is well suited for many-particle coincidence measurements in ionizing collisions. First experimental results for fast ion and electron impact on helium targets are presented. Future applications in atomic collision physics and related areas are discussed.

Key Words: *recoil-ion momentum spectroscopy, high-resolution translational spectroscopy, cold supersonic jet targets, complete measurement of the momentum balance in ionizing collisions*

INTRODUCTION

A novel technique for high-resolution momentum spectroscopy is presented, which allows for the first time a precision measurement of the complete momentum balance in ionizing ion–atom collisions. Using cold supersonic jet or laser cooled atomic targets, the

Comments At. Mol. Phys.
1994, Vol. 30, No. 5, pp. 285–304
Reprints available directly from the publisher
Photocopying permitted by license only

initial target state is extremely well prepared ($T = 30$ mK) and thus the momentum transfers Δp during the encounter with any kind of projectile can be determined with an accuracy exceeding $\Delta p/p = 10^{-8}$ for selected systems, still achieving a detection efficiency of nearly 100%. p is the projectile initial momentum in the laboratory system.

In atomic physics, so far high-resolution techniques have mainly been restricted to the spectroscopy of electronic transition energies and energy levels, i.e., to the investigation of the stationary electronic structure of atoms and ions or even exotic systems like muonic atoms, geonium, heavy few electron ions, etc. In these investigations an impressive experimental precision has been reached using high-resolution photon and electron spectrometers, advanced maser and laser techniques, traps and storage rings, leading to a very profound theoretical understanding of the electronic level structure of stationary systems including contributions due to relativistic, QED, electroweak and even QCD effects.[1–10]

In contrast, the understanding of dynamic processes in atomic collisions has been seriously lagging behind due to enormous theoretical problems in describing time-dependent many-particle reactions and due to the huge basic difficulties in performing "complete" scattering experiments in atomic physics. Only recently has considerable theoretical progress been achieved in treating the dynamical three-body Coulomb problem.[11–14] Furthermore first experiments have been performed where two continuum electrons were detected in coincidence for the double photoionization of rare gases.[15,16] However, applying conventional electron spectroscopy, an improvement of resolution causes a reduction of detection solid angle. Therefore electron–electron coincidence measurements can only be performed for selected collision systems, where the cross sections are sufficiently high.

The novel technique described in this paper, for the first time allows us to detect one reaction product, namely the recoiling target ion, with very high momentum resolution of $\Delta p = 0.05$ a.u., still achieving a detection efficiency close to 100%. This momentum resolution corresponds to an energy resolution of $\Delta E = 40$ meV in the electron detection channel. Notice that the solid angles of con-

ventional electron spectrometers with such an energy resolution are typically below 10^{-4} sterad. Thus gaining a factor 10^{+5} in solid angle Cold Target Recoil Ion Momentum Spectroscopy (COLTRIMS) will enable a new generation of precision experiments in atomic collision physics and related areas: Applying multi-coincidence techniques between the recoil ion and emitted photons or electrons, kinematically complete experiments can be envisaged, investing double and multiple target ionization, projectile ionization and excitation as well as electron capture (radiative or kinematical) in so far unachieved detail and precision. In contrast to conventional translational spectroscopy, the resolution depends only to second order on the momentum spread of the incoming projectile and does not decrease with increasing projectile velocity. The new technique is, in particular, applicable in GeV collisions or in storage rings.

COLTRIMS marks an important step forward compared to the traditional recoil-ion detection methods (see, e.g., Refs. 17–21), which have been used in numerous experimental investigations to study ionization and capture reactions. In first generation experiments, the final recoil-ion charge state was detected in coincidence with other reaction products, revealing cross sections integrated over all impact parameters. With improved techniques in second generation experiments, either the recoil ion transverse[21–24] or longitudinal[25–28] momenta were measured with a typical resolution of a few a.u., thus yielding detailed information on the transverse momentum balances, impact parameter dependencies or on the Q-value (inelasticity) of the reaction. In this paper the third generation recoil-ion spectrometers are presented. A short description of the basic features of COLTRIMS is given together with a compressed presentation of first results and possible applications and future perspectives.

To control experimentally the complete momentum balance in an ionization process (with a non-zero Q-value), where the projectile P (ion, electron, photon, etc.) hits a cold target atom T and n initially bound electrons are emitted into continuum states, m final momentum components have to be determined. The number of m is equal to the number of $(n+2) \times 3$ final momentum components

plus 1 (unknown Q-value) reduced by 4 [because of energy (reduction of 1) and momentum (reduction of 3) conservation]. If $n = 0$ (projectile or target excitation only), it is sufficient to measure the three recoil-ion momentum components to identify the complete momentum balance and simultaneously the Q-value of the reaction. If $n = 1$ (single ionization of projectile or target, e.g., an (e,2e) reaction), in addition to the recoil-ion momentum vector, also two electron or projectile momentum components must be measured. Thus adding the appropriate position-sensitive electron or projectile detectors to the recoil-ion detection system, the required complete momentum determination can be achieved.

EXPERIMENTAL TECHNIQUE OF COLTRIMS

COLTRIMS is based on a *very cold, thin, and localized supersonic gas jet* traversing a well controlled electrostatic field configuration. In Fig. 1 the experimental set-up is presented in a schematic way. The rare gas (He, Ne, Ar, etc.) is precooled to a temperature of approximately 15 K (for He) at a pressure of between 200 and 1000 mbar using the cold head of a cryopump. The precooled gas expands through a 30 micrometer hole forming a very cold supersonic jet. The coolest inner jet fraction passes through a 0.3 mm skimmer into the scattering chamber. For He this final jet has a transverse temperature of about 0.04 a.u. The longitudinal momentum spread is about 0.03 a.u. The jet diameter at the intersection point with the fast ion, electron or photon beam is 1.1 mm. Depending on the actual reaction investigated, an appropriate weak homogeneous electrostatic field in the acceleration region (optimized for resolution and detection efficiency) bends practically all recoil ions of interest towards the drift region (see Fig. 2). After passing the drift region, the ions are detected by a two-dimensional position-sensitive channel plate detector. Knowing the electrostatic field, the position where the ionization event took place (projectile–target intersection), the final detection position and the recoil-ion time-of-flight (TOF), its trajectory can be calculated. From the recoil-ion trajectory and its TOF, the recoil-ion mo-

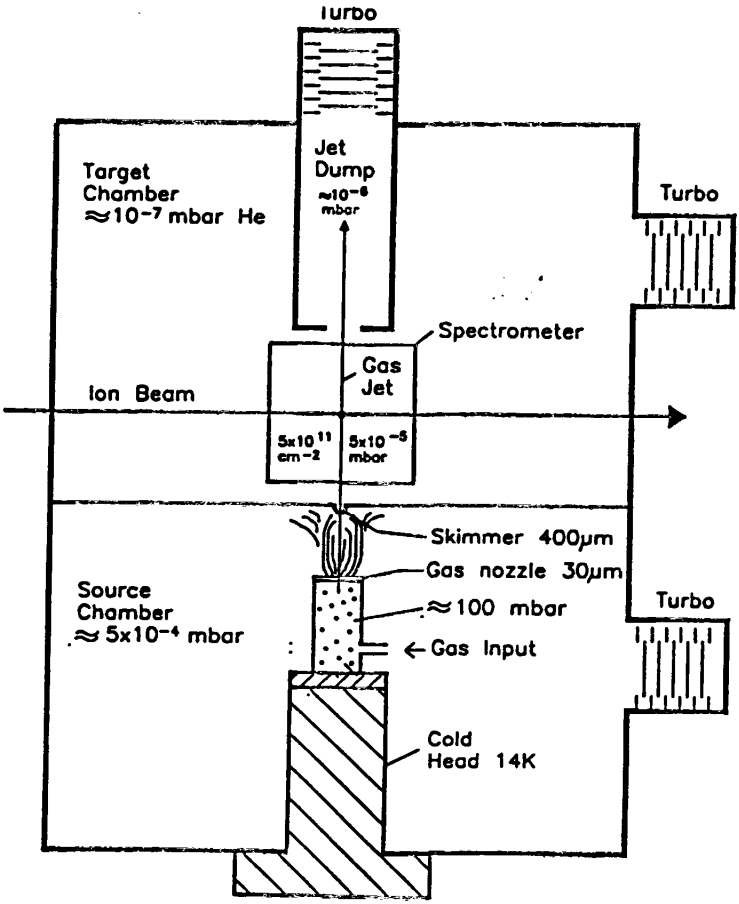

FIGURE 1 Schematic presentation of the experimental set-up. The lower part shows the cooled head with gas reservoir and the gas expansion hole, the upper part (separated by the skimmer) the recoil-ion spectrometer and the gas jet dump. The effective jet density at the intersection point with the projectile beam is given also (5×10^{-5} Torr corresponds to 5×10^{11} atoms/cm^2 target thickness at about 14 K).

mentum vector is absolutely determined with a relative accuracy of better than 0.5%. In order to obtain an optimum momentum resolution for all three momentum components (p_x, p_y, p_z), the size of the intersection area of gas jet and projectile beam has to be mini-

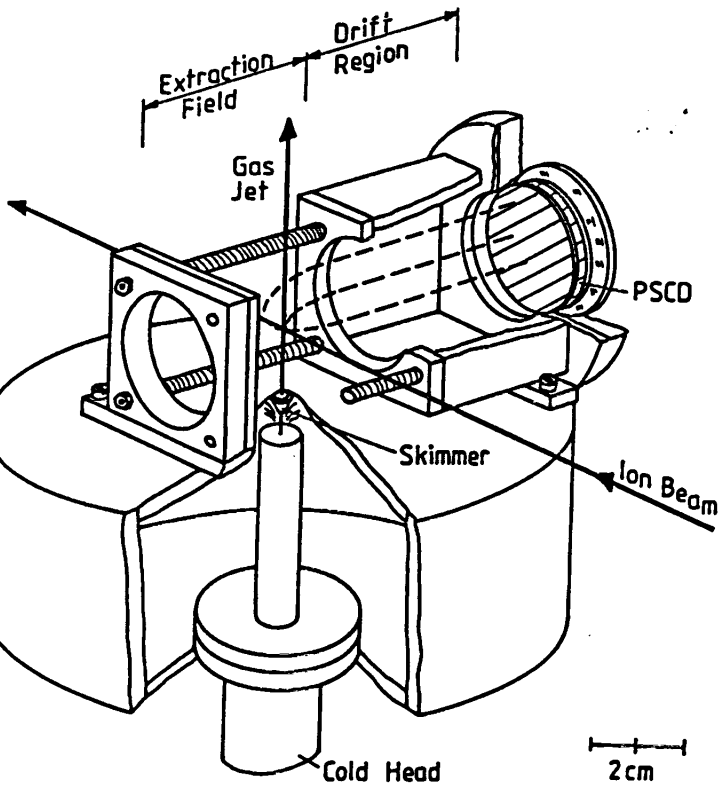

FIGURE 2 Present recoil-ion spectrometer device. The ion beam intersects the gas jet in the extraction field region. After penetration of the drift region, the recoil ions are detected on the position-sensitive channel plate detector (PSCD).

mal. In the x and y directions a very narrow projectile beam collimation (typically 0.1×0.1 mm^2) ensures the very precise determination of the x and y recoil momentum components. In the z direction the resolution is primarily limited by the 1.1 mm width of the target gas jet. However, using the time focusing field geometry along the z axis (i.e., extract the recoil ions with a field in the z direction with a ratio of path length in the extraction field to that in the drift region of 0.5), the "poor" resolution in the z component

due to the jet width can be eliminated to first order. In this way a very good momentum resolution comparable to the one in the x and y directions can be achieved, too.[29,30]

For a complete determination of the total momentum balance in an ionizing collision, the emission angles (two momentum components) of the ejected electrons must additionally be measured. Thus position-sensitive electron detectors have to be placed around the open recoil-ion extraction region, providing an optimum detection efficiency of several sterads and the required resolution. The influence of the weak electrostatic field on the electron trajectory can be precisely calculated. For two or more electron coincidence experiments, total coincidence efficiencies of a few % can be obtained by using large area position-sensitive channel plate detectors with multi-hit capability.[31,32]

SELECTED EXPERIMENTAL RESULTS

To demonstrate the power of COLTRIMS, first experimental data for three typical ionization reactions will be presented:

(i) Electron capture: 0.25 MeV He^{2+} on $He \rightarrow He^{*1+} + He^{*1+}$;
(ii) Projectile ionization: 0.25 to 2 MeV He^{1+} on $He \rightarrow He^{2+} + He^{1+} + 2e$;
(iii) Target ionization: 500 eV electron on $He \rightarrow He^{1+} + 2e$.

(i) Electron Capture: 0.25 MeV $He^{2+} + He \rightarrow He^{*1+} + He^{*1+}$

This electron capture process[32] is a pure two-body reaction, and the measurement of all three recoil-ion momenta allows us to determine the complete momentum balance including the Q-value of the reaction, i.e., the identification of excited states. For small scattering angles (perfectly fulfilled in this case), we obtain from momentum and energy conservation for the final recoil ion longitudinal $p_{\parallel R}$ and transverse $p_{\perp R}$ momenta, respectively (the initial target atom momentum is zero!).

$$p_{\parallel R} = -Q/v_p - mv_p/2, \tag{1a}$$

$$p_{\perp R} = -p_{\perp p} = -p_0 \sin\theta_p . \tag{1b}$$

v_p and p_0 are the projectile initial velocity and momentum, respectively. For the present collision system: $v_0 = 2.23$ a.u. and $p_0 = 1.6 \times 10^{+4}$ a.u. Notice that in this limit of small center-of-mass angles, both momentum components are completely independent of each other, thus allowing a precise determination of both the nuclear trajectory and of the Q-value of the electronic transitions (for details see Refs. 25 and 29). The $mv_p/2$ term in Eq. (1a) accounts for the electron mass transfer from the target to the projectile, which yields a backward momentum component of the recoil ion in the laboratory system. The recoil-ion transverse momentum must be identical to the projectile transverse momentum, i.e., corresponds to the projectile scattering angle. With the resolution obtained in this experiment of $p_{\parallel R} = \pm 0.13$ a.u. and $p_{\perp R} = \pm 0.025$ a.u., a Q-value resolution of about ± 8 eV and a scattering angle resolution of about $\pm 3 \times 10^{-6}$ rad is achieved. The recoil-ion time-of-flight and the capture reaction are identified by a coincidence between the outgoing He^{1+} projectiles and the He^{1+} recoil ions. In Fig. 3 the measured differential cross sections are presented. Electron capture into the projectile K-shell (left peak) is clearly separated from the capture into the L-shell, or K-shell capture plus simultaneous target excitation (right peak). These results show that COLTRIMS for the first time allows the direct measurement of differential cross sections for single capture into excited states at such a high projectile velocity. With the present resolution, even high n states, up to $n = 20$, would be separable for 10 MeV/u U on He collisions,[29] which corresponds to a Q-value resolution of about 10^{-8}. This value can be improved by extracting the recoil ions along the beam direction.[33]

Particularly in storage rings, COLTRIMS is a powerful method since the projectile beam is not affected, and it can be applied to study multiply differential state selective capture cross sections. According to Eq. (1a) the Q-value of the reaction can directly be determined from the longitudinal recoil-ion momentum compo-

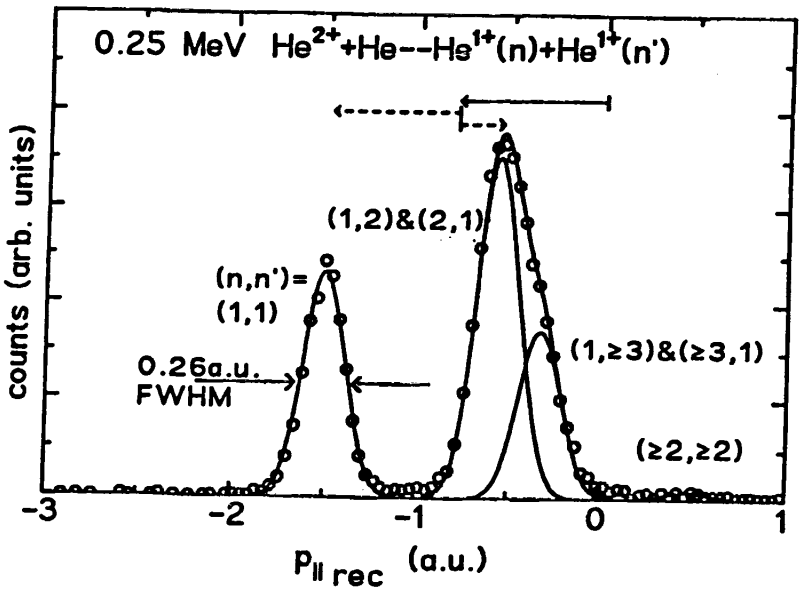

FIGURE 3 Longitudinal momentum distribution for recoil ions from the single electron capture reaction 0.25 MeV $He^{2+} + He \rightarrow He^{*1+} + He^{*1+}$. The different peaks correspond to different capture states (n and n' indicate the final main quantum numbers of the electrons in the projectile and the target, respectively). The arrows above the right peak represent the momenta (i) (solid line) due to the mass transfer of the electron from target to the projectile (term $mv_p/2$ in Eq. (1a)) and (ii) (dashed lines) due to the different excitation energies of the final electron states (term Q/v_p in Eq. (1a)). The experimental resolution is given for the left peak.

nent. However, due to the large transverse momentum transfers in close inner shell capture collisions, these transverse momenta would affect the precision of the $p_\parallel$ measurement. Applying a magnetic solenoid field in the z direction, the transverse momentum component just leads to a helix path along the z direction, allowing a precise recoil-ion time-of-flight measurement in the z direction and thus a precise $p_\parallel$ determination. The Q-value resolution achieved with the present set-up would correspond to a linewidth (FWHM) of about 100 eV for the determination of the uranium K-shell binding energy in 5 MeV/u U^{92+} on He single capture collisions. This is already about a factor of 10 better than the best results

obtained with solid-state x-ray detectors. Applying the "time-focusing" geometry, a FWHM of about 20 eV can be envisaged, making COLTRIMS a high resolution energy spectroscopy instrument. In such a configuration the longitudinal momentum is determined with high precision, whereas the transverse momentum (i.e., impact parameter) is measured only on the 10% level. Because of the very high luminosity of the GSI experimental storage ring (ESR) and the 4π detection solid angle of the solenoid device, mbarn capture cross sections become accessible with COLTRIMS. First experiments with solenoid coils have been successfully performed at the UNILAC of GSI.[33]

(ii) Projectile Ionization: He^{+1} on He $\rightarrow$ He^{2+} + He^{1+}

In this reaction[34] the projectile as well as the target are simultaneously ionized where the ionization can proceed either via *electron–nucleus (e-n) or via electron–electron (e-e) interaction.* The e-e collisions will in general occur at larger impact parameters, leading to smaller recoil-ion transverse momenta than e-n encounters.[34–38] In the case of e-e interaction the target nucleus is mostly just a spectator, remaining in its initial momentum state. The e-n ionization, however, will lead in general to larger transverse recoil momenta, and the longitudinal recoil momentum will directly reflect the Q-value of the reaction. Thus we expect different recoil-ion momentum patterns for both processes which might be separable by using COLTRIMS. In Fig. 4c the measured recoil momentum distribution is shown for $E_p = 1$ MeV. To identify the projectile ionization experimentally, the recoil ions were measured in coincidence with the outgoing He^{2+} projectiles. Two maxima are visible in the contour plot. The first maximum (×) (smaller recoil-ion momenta) reflects the e-e contribution and the second maximum (+) the e-n interaction. To manifest this statement, the corresponding recoil momentum distribution for 130 eV electron impact has been measured, too (see Fig. 4f). These electrons have the same impact velocity as 1 MeV He^{1+} ions. The maximum position (×) coincides exactly with the one of electron impact.

Further evidence for the above interpretation is provided by the measured projectile energy dependence, which is shown in Figs. 4a–e. The e-e contribution displays a threshold behavior (threshold for pure e-e ionization is $E_p = 400$ keV). Above the threshold a weaker E_p dependence than for the e-n reaction is expected. According to Ref. 34 the e-n contribution will decrease with E_p^{-2} (two-step process) and the e-e contribution (one-step process) only with $1/E_p$. Figure 4 demonstrates that COLTRIMS has the power to separate experimentally in a clear kinematic manner the small differences in the momentum transfers between e-e and e-n scattering in bound many-particle systems.

Thus we can expect that COLTRIMS will allow the measurement of impact parameter dependent cross sections for single and multiple excitation and ionization of heavy few-electron systems up to hydrogen-, helium- or lithium-like uranium projectiles in the ESR storage ring in collisions with rare gas targets. From the experimental results at lower energies and for light projectiles presented in this paper, it can be concluded that contributions due to e-e or e-n interactions will be clearly separated. Such experiments, which are in preparation, will mark an important step forward compared to total cross section measurements.

(iii) Electron Impact Target Ionization[40]: 500 eV $e + He \rightarrow e + He^{1+} + e$

(e,2e) reactions have been systematically investigated by electron–electron coincidence techniques (for a review see, e.g., Ref. 41). Measuring the two final electron momentum vectors, the complete momentum balance in the final state is known for single ionization. Due to experimental difficulties (small spectrometer solid angles, etc.), however, so far mostly coplanar electron momenta (momentum vector of incoming and both final electrons in one plane) have been investigated.[42] In the future COLTRIMS will allow the complete measurement of all momenta without any spatial restriction with high efficiency and good resolution. Using the setup shown in Fig. 2, all three recoil momenta are measured with about 4 π solid angle. Two momentum components of the fast elec-

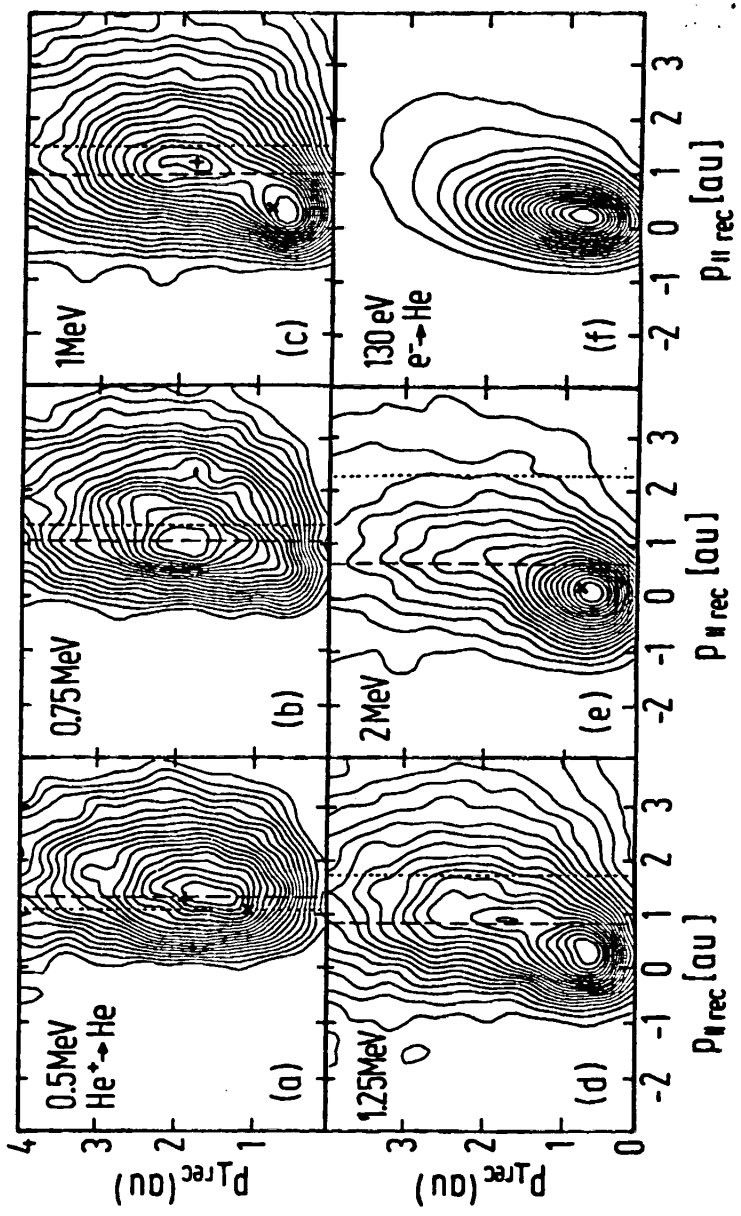
0.5MeV
He+→He
(a)
0.75MeV
(b)
1MeV
(c)
1.25MeV
(d)
2MeV
(e)
130eV
e⁻→He
(f)
p⊥rec (au)
p∥rec [au]

tron are measured with high efficiency by a position-sensitive detector mounted in the forward direction. The position of the second electron is measured by a second position-sensitive electron detector mounted under 90 degree with respect to the beam direction. Thus seven out of nine final momenta become experimentally accessible. Such experiments are presently underway.[43] Adding one more position-sensitive electron detector, kinematically complete investigations of even (e,3e) reactions can be envisaged with an overall coincidence efficiency of about 1%.

So far, for electron impact, only the recoil momentum and charge state have been measured with COLTRIMS without any electron coincidence. These data already give new insight and interesting information on the (e,2e) and particularly on (e,3e) processes. In Fig. 5 for 500 eV electrons on He, the single differential cross sections $d\sigma/dp$ for He-single ionization as a function of the recoil-ion momentum are presented in comparison with CTMC calculations and measured cross sections as a function of the final electron energy. A quantitative comparison[40] of these recoil-ion data with the Compton profile given in the literature[44] shows that the final recoil-ion momentum distribution after such collisions is even narrower than the initial recoil-ion Compton profile. In Fig. 6 the measured recoil-ion momentum distribution ($p_{\perp R}$ and $p_{\parallel R}$) is shown for He^{2+} ions. It is obvious from these data that for He^{2+} there is practically no contribution with $p_R = 0$, i.e., ionization at the BETHE ridge[12,13] is found to be negligibly small. For He-double ionization, however, a clear signature of the incoming electron–nucleus scattering is observed. The two-body momentum exchange between these two particles is indicated by the solid line in the figures. Details on this measurement and on the interpretation of the data are given in Ref. 40.

FIGURE 4 Transverse and longitudinal recoil-ion momentum distributions (linear contour plots) for the $He^{1+} + He \rightarrow He^{2+} + He^{1+}$ ionization reaction. (a) (He^{1+} impact) and (b) (electron impact) correspond to the same projectile velocity (see text). The long dashed line marks the estimated $p_{\parallel R}$ peak position of the e-n process and the short dashed line the peak position of the e-e process. The + and × mark the corresponding maxima of the CTMC calculations (Ref. 34).

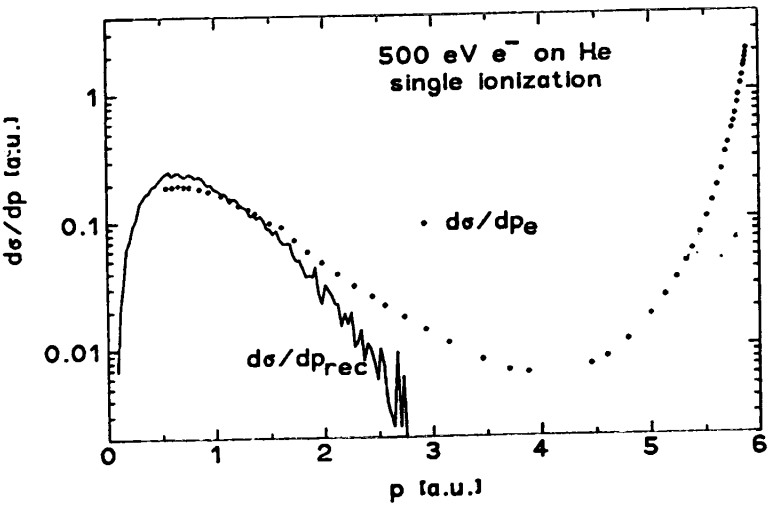

FIGURE 5 Differential cross sections ($d\sigma/dp$) for He single ionization as function of the recoil-ion momentum (p_R) for 500 eV electron impact (solid line). The dotted line represents the corresponding differential cross sections as functions of the final electron momentum. Since the fast primary and the slow ionization electrons cannot experimentally be distinguished, the electron distribution must show the double peak structure (Ref. 40).

SUMMARY AND FUTURE PERSPECTIVES

In the previous section we have demonstrated the potential of COLTRIMS which combines three important features in a unique way: (1) high momentum resolution, (2) nearly 100% detection efficiency for the recoil ions and (3) the "open" construction geometry supporting easy implementation of electron or photon detectors for a multi-coincidence system. We have presented selected examples on electron capture, projectile ionization and target single and double ionization by ion and electron impact. They illustrate the power of COLTRIMS to illuminate the mechanisms of collision induced many-body momentum transfers. In addition to some future developments which have already been mentioned, several other perspectives will be considered in this section.

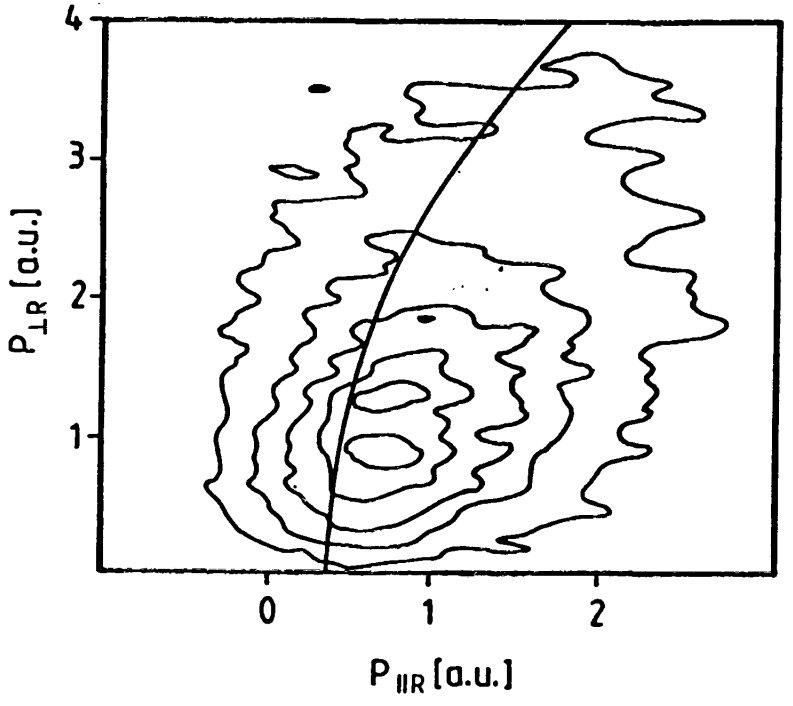

FIGURE 6 Contour plot (linear scale) of differential cross sections of He double ionization for 500 eV electron impact on He as a function of the recoil-ion transverse and longitudinal momenta. The solid line indicates the recoil-ion momentum distribution for a pure two-body (fast-electron nucleus) collision.

1. Photoionization, Multi-Photon Ionization and Compton Scattering

The cross section for single ionization of target atoms by high-energy photon impact is very small and typically in the barn regime. Thus measurements investigating multiple photoionization or Compton scattering on gas-target atoms are facing tremendous experimental difficulties. So far only two experiments on rare gas double ionization at low photon energy have been reported[15,16] re-

cently where two outgoing electrons have been analysed in coincidence. Due to the small solid angle of the electron spectrometers, the electrons were only detected under special geometrical conditions (both electrons have fixed and identical final velocity and were coplanar with the incoming photon). Typical count rates are on the order of 1000 per day. Thus the low coincidence detection efficiencies of conventional methods prohibit a study of the complete momentum balance for photoionization at high (keV regime) photon energies. The situation is similar for helium double ionization in intense laser fields (multi-photon ionization) and Compton scattering of high energy photons (above 5 keV) on gaseous targets, where so far no experiment has been performed.

Combining COLTRIMS with position-sensitive electron detectors, the overall coincidence detection efficiency of such experiments can be increased by more than 5 orders of magnitude as compared to an e-e coincidence experiment still having very good momentum resolution. Even in a "singles" experiment (no coincidence with electrons or photons), the photo-effect and Compton-effect contributions to the helium double ionization can easily be separated from the recoil-ion momentum distribution. For photoionization the recoil ion has to compensate the momentum of the primary fast electron. In this case, e.g., for 8 keV photon impact, the recoil momentum for He-double ionization is approximately 24 a.u. For double ionization after Compton scattering, the recoil ion is a "spectator" and its momentum is close to 2 a.u. only. Experiments to study these processes in detail have just recently been performed at Hasylab (Desy–Hamburg) and are in preparation at the ALS (LBL–Berkeley).[45]

2. Electron–Neutrino Angular Correlation and Neutrino Mass Measurements in β-Decay

The first indirect experimental evidence for neutrino existence was achieved in 1952 by Rodeback and Allen, measuring the 9.6 eV recoil energy of ^{37}Cl from the monoenergetic neutrino emerging after β-decay of ^{37}Ar by electron capture from the K shell.[46] The

recoil energy was determined by a time-of-flight measurement of ^{37}Cl using the Cl-K-Auger electron as a start signal.

In an improved experiment using COLTRIMS for the recoil-ion momentum measurement and large area position-sensitive electron detectors, the angular correlation between the recoil ion and electron, and thus the angular correlation between the electron and the remaining neutrino, can be studied with high resolution. So far only very few so-called angular correlation measurements between electron and neutrino have been performed for quite energetic recoiling nuclei (MeV regime), where only the left-right or forward-backward anisotropies were investigated. If polarized nuclei decay, these anisotropies yield basic information on invariance rules in the weak interaction.[47] Also, high-resolution experiments could provide new unexpected structure in the angular distributions due to coherent superposition of the different decay channels (Thomas–Fermi or Gamow–Teller transitions). Investigating the tritium β-decay with a 50 cm long recoil-ion detection system, a neutrino-momentum resolution of about 50 eV/c = 0.014 a.u. can be achieved. In a second generation COLTRIMS set-up using laser cooled tritium targets and measuring, in addition, the electron energy (longitudinal electron momentum), the neutrino mass can be determined in principle from each single detected event. A precision below 10 eV should be obtainable, depending on the size of the recoil-ion and electron drift lengths. In such an experiment, six momentum components are measured instead of one (electron energy), as the conventional methods do. Thus all other contributions to the Q-value resulting from molecular or solid state effects are controlled in a clean way, which is a serious problem of the present investigations.

3. High-Precision Measurement of Photon Energies

Another quite unusual but interesting application of COLTRIMS is the very precise x-ray energy measurement. In a photoionization event the total photon energy is equal to the He-1s-electron binding energy plus the kinetic energy of the ejected photo-electron and the He^{1+} recoil ion. Measuring precisely the recoil-ion momentum,

the total kinetic energy of the recoil ion and the electron can be accurately determined. Precision in the recoil-ion time-of-flight of 10^{-4} can be achieved, and thus the photon energy will be obtained with a high resolution just measuring a TOF interval by electron-recoil-ion coincidence. The ultimate relative photon energy resolution is given by the mean target momentum spread (about 0.03 a.u.) divided by the final recoil momentum. For 1 keV photons the recoil-ion momentum is about 8.5 a.u. and a photon-energy resolution of $\Delta E/E = 1$eV is expected. Such a technique could be used for calibrations of the synchroton radiation energy. Since COLTRIMS is a very new experimental spectroscopy technique, more applications will certainly come up in the near future. This article is only a short introduction to recent developments and first results using such cold supersonic gas-jet targets in the field of recoil-ion momentum spectroscopy.

Acknowledgments

Although COLTRIMS is a new technique in the field of atomic collision physics, its development from first generation recoil-ion spectrometers to the present high-resolution system has lasted about a decade. During this time we had numerous very helpful discussions with our colleagues and friends. In particular we want to thank C. L. Cocke, R. E. Olson, U. Buck, R. Dreizler, M. Horbatsch and S. Hagmann.

J. ULLRICH
GSI-Darmstadt,
64291 Darmstadt, Germany

R. DÖRNER, V. MERGEL, O. JAGUTZKI,
L. SPIELBERGER and H. SCHMIDT-BÖCKING
**Institut für Kernphysik der Universität Frankfurt,*
60486 Frankfurt, Germany

References

1. T. Andreae, Phys. Rev. Lett. **68**, 1923 (1992).
2. M. Weitz, F. Schmidt-Kaler and T. W. Hänsch, Phys. Rev. Lett. **68** (1992).

*Supported by DFG, GSI and BMFT.

3. H. Dehmelt, Rev. Mod. Phys. **62**, 525 (1990).
4. N. F. Ramsey, Rev. Mod. Phys. **62**, 541 (1990).
5. W. M. Itano, J. C. Bergquist, R. G. Hulet and D. J. Winieland, Physica Scripta **T22**, 79 (1988).
6. Th. Stöhlker *et al.*, Phys. Rev. Lett. **71**, 2184 (1993).
7. M. Siegbahn, *Spectroscopy of X-Rays* (Oxford University Press, London, 1925).
8. W. R. Johnson and G. Soff, At. Data Nucl. Data Tables **33**, 405 (1985).
9. P. J. Mohr and G. Soff, Phys. Rev. Lett. **70**, 158 (1993).
10. G. Werth, Physica Scripta **T22**, 191 (1987).
11. J. S. Briggs, in *The Physics of Electronic and Atomic Collisions*, page 221, eds. T. Andersen *et al.* (AIP, New York, 1993).
12. J. Berakdar and H. Klar, J. Phys. **B26**, 3891–913, 4219–35 (1993).
13. W. Fritsch and C. D. Lin, Phys. Rev. Lett. **61**, 690–93 (1988).
14. M. Brauner, J. S. Briggs and H. Klar, J. Phys. **B22**, 2265 (1989).
15. O. Schwarzkopf, B. Krässig, J. Elmiger and V. Schmidt, Phys. Rev. Lett. **70**, 3008 (1993).
16. A. Huetz, P. Lablanquie, L. Andric, P. Selles and J. Mazeau, J. Phys. **B27**, L13 (1994).
17. C. L. Cocke and R. E. Olson, Physics Reports **205**, 155 (1991).
18. C. Kelbch, J. Ullrich, R. Mann, P. Richard and H. Schmidt-Böcking, J. Phys. **18**, 323 (1985).
19. A. Müller, B. Schuch, W. Groh, E. Salzborn, H. F. Beyer, P. Mokler and R. E. Olson, Phys. Rev. **A33**, 3010 (1986).
20. J. Ullrich *et al.*, Phys. Rev. Lett. **71**, 1697 (1993).
21. J. Ullrich, H. Schmidt-Böcking and C. Kelbch, Nucl. Instr. Meth. **A268**, 216 (1988).
22. R. Dörner, J. Ullrich, H. Schmidt-Böcking and R. E. Olson, Phys. Rev. Lett. **63**, 147 (1989).
23. A. Gensmantel, J. Ullrich, R. Dörner, R. E. Olson, K. Ullmann, E. Forberich, S. Lencinas and H. Schmidt-Böcking, Phys. Rev. **A45**(7), 4572–75 (1992).
24. R. Dörner, J. Ullrich, R. E. Olson, O. Jagutzki and H. Schmidt-Böcking, Phys. Rev. **A47**, 3845 (1993).
25. R. Ali, V. Frohne, C. L. Cocke, M. Stöckli and M. L. A. Raphaelian, Phys. Rev. Lett. **69**(17), 2491–94 (1992).
26. V. Frohne, S. Cheng, R. Ali, M. Raphaeilian, C. L. Cocke and R. E. Olson, Phys. Rev. Lett. **71**(5), 696–699 (1993).
27. R. Dörner, J. Ullrich, O. Jagutzki, S. Lencinas, A. Gensmantel and H. Schmidt-Böcking, in W. R. MacGillivray, I. E. McCarthy and M. C. Standage, editors, *Electronic and Atomic Collisions, Invited Papers of the ICPEAC XVII*, page 351 (Adam Hilger, 1991).
28. C. L. Cocke, in D. Bereny and G. Hock, editors, *Lecture Notes in Physics*, page 253 (Springer-Verlag, 1990).
29. V. Mergel, Diploma thesis Universität Frankfurt, unpublished (1994).
30. V. Mergel *et al.*, Phys. Rev. Lett., submitted (1994).
31. R. Moshammer, GSI Scientific Report (1993).
32. S. Nuettgens, Master's thesis, Universtät Frankfurt/Main (1994).
33. R. Moshammer *et al.*, submitted to Phys. Rev. Lett.
34. R. Dörner *et al.*, Phys. Rev. Lett. **72**, 3166 (1994).
35. E. C. Montenegro and W. E. Meyerhof, Phys. Rev. **A46**, 5506 (1992).
36. W. Fritsch and C. D. Lin, contributed paper to the XVIII ICPEAC, 1993, page 452, Eds. T. Andersen *et al.* (ISBN87-8754834-8), Aarhus University, Aarhus.
37. N. M. Kabachnik, J. Phys. **26**, 3803 (1993).
38. W. Wu *et al.*, Phys. Rev. Lett. **72**, 3170 (1994).

39. O. Jagutzki, PhD Thesis, University Frankfurt (1994).
40. O. Jagutzki *et al.*, submitted for publication (1994).
41. A. Lahmam-Bennani, J. Phys. **B24**, 2401 (1991).
42. H. Ehrhardt, K. Jung, G. Knoth and P. Schlemmer, Z. Phys. **D1**, 3 (1986).
43. L. Spielberger, O. Jagutzki, R. Dörner, K. Froschauer, A. Gensmantel, H. Schmidt-Böcking, J. Ullrich and U. Buck, in C. T. Whelan *et al.*, editors, *(e,2e) and Related Processes*, pages 119–129 (Kluwer Academic Publishers, 1993).
44. P. Eisenberg, Phys. Rev. **A2**, 1678 (1970).
45. V. Mergel *et al.*, to be published (1994).
46. G. W. Rodeback and J. S. Allen, Phys. Rev. **86**, 446 (1952).
47. A. L. Hallin, F. P. Calaprice, D. W. MacArthur, L. E. Piilonen, M. B. Schneider and D. F. Schreiber, Phys. Rev. Lett. **52**, 337 (1984).